Quarterly Journal of the Royal Meteorological Society
A journal of the atmospheric sciences and physical oceanography
RMetS

The Horizontal and Vertical Controls on the Thermal Structure of the Tropical Troposphere

Journal:	*QJRMS*
Manuscript ID	QJ-24-0016
Wiley - Manuscript type:	Research Article
Date Submitted by the Author:	23-Jan-2024
Complete List of Authors:	Palmer, Lucinda; Monash University, School of Earth, Atmosphere and Environment Singh, Martin; Monash University, School of Earth, Atmosphere and Environment
Keywords:	Convection < 3. Physical phenomenon, quasi-equilibrium, weak temperature gradient, tropical stability, entrainment
Country Keywords:	AAA - No country

ORIGINAL ARTICLE

Journal Section

The Horizontal and Vertical Controls on the Thermal Structure of the Tropical Troposphere

L. A. Palmer[1,2] | **M. S. Singh**[1,2]

[1]School of Earth, Atmosphere, and Environment, Monash University, Melbourne, VIC, Australia

[2]Centre of Excellence for Climate Extremes, Monash University, Melbourne, VIC, Australia

Correspondence
L. A. Palmer, School of Earth, Atmosphere and Environment, Monash University, Melbourne, VIC, Australia
Email: lucinda.palmer@monash.edu

Funding information
Australian Research Council, Grant Numbers: DE190100866 and DP230102077; Centre of Excellence for Climate Extremes, Grant Number: CE170100023

Our conceptual understanding of the tropical thermal structure is based on two complementary idealisations: convective quasi-equilibrium (QE) and the weak-temperature gradient (WTG) approximation. Through QE, moist convection provides a local vertical control on the thermal structure, while under WTG, wave dynamics are assumed to provide a non-local horizontal control. While it is clear that moist convection plays an important role in setting the tropical mean stability through QE, the extent to which it applies locally in different regions or whether the requirement for WTG effectively inhibits the influence of local conditions on stability remains debated. Here we hypothesise that a strong local vertical control of the thermal structure would imply a relationship between humidity and stability in the troposphere, as convection within moister regions would be less affected by entrainment of surrounding air. We utilise a combination of ERA5 reanalysis and observational data to examine the relationship between stability and local humidity across the tropics. The results are compared to a prediction based upon a modified version of the theory of QE that incorporates entrainment through a simple plume model. We discover that, in convective regions, moist convection is most influential and that the resulting relationship between stability and humidity can be well approximated by the entraining plume model. However, in non-convective regions,

QE cannot be used to explain the thermal structure and instead the WTG, and possibly other factors, act to set stability in the region. These results may help us understand the controls on horizontal density gradients in the tropical troposphere and the associated overturning circulations.

KEYWORDS
convection, quasi-equilibrium, weak temperature gradient, tropical stability, entrainment

1 | INTRODUCTION

In the tropics there are two key idealisations that ground theoretical understanding of the thermal structure of the troposphere (Bao and Stevens, 2021). The first of these is the assumption that horizontal variations in free-tropospheric temperature are small. This stems from what is known as the weak-temperature gradient (WTG) approximation (Sobel et al., 2001): since the influence of rotation in the tropics is weak, gravity waves are able to efficiently remove density anomalies in the tropical troposphere (Bretherton and Smolarkiewicz, 1989), preventing strong temperature gradients from being maintained (Charney, 1963). The second idealisation, known as convective quasi-equilibrium (QE), states that, in regions of convection within the tropics, the thermal structure follows that of moist adiabatic ascent (Betts, 1982; Xu and Emanuel, 1989). Together, these assumptions provide a simple picture of the tropical troposphere as having a horizontally homogeneous temperature with a profile close to that of a moist adiabat. It is important, however, to note that both these principles are approximations; research has shown that substantial horizontal gradients in temperature do exist in the tropical troposphere (Bao and Stevens, 2021) and that the thermal structure does not necessarily adhere strictly to a moist adiabat (Mapes, 2001). Therefore, an important challenge in tropical meteorology is to understand the causes and implications of deviations from QE and WTG in the observed thermal structure.

The processes that maintain weak temperature gradients within the tropical troposphere include wave dynamics that spread the effect of diabatic heating horizontally (Bretherton and Smolarkiewicz, 1989). Such mechanisms therefore provide a horizontal control on the tropical thermodynamic structure, that acts non-locally to reduce density anomalies. However, this does not lead to perfect homogenisation of temperature (Fig. 1). Firstly, due to the virtual effect of water vapour, even when density is horizontally invariant, temperature variations can exist due to horizontal variations in moisture (Yang et al., 2022). Moreover, the existence of large-scale overturning circulations imply non-zero density gradients in the free troposphere. For example, (Bao and Stevens, 2021) showed that temperature variations (and density temperature variations) of 2-4 K are present seasonally in the upper tropical troposphere and could be related hydrostatically to pressure gradients required to maintain the circulation. Indeed, in studies that apply the WTG approximation to limited-area modelling, temperature anomalies are either implicitly (Kuang, 2008) or explicitly (Raymond and Zeng, 2005) related to large-scale vertical motion. Bao and Stevens (2021) found that the magnitude of the temperature anomalies were smallest in the mid-troposphere, suggesting the efficacy of gravity waves in homogenising the density is greatest in the mid-troposphere.

To understand deviations from strict WTG, Williams et al. (2023) introduced the conceptual "Circus Tents" model of the free-tropospheric temperature. In this model, temperature in the free-troposphere is maintained through moist adiabatic ascent in deep convective regions (the tent poles) and slowly decreases with distance from deep convection (the tent fabric) due to the imperfect efficacy of gravity waves in removing density gradients. The model therefore

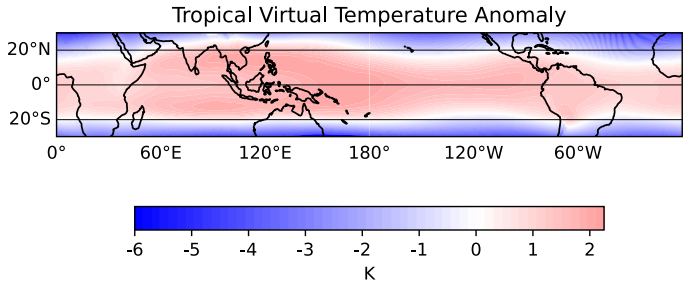

FIGURE 1 The time-mean virtual temperature anomaly at 500 hPa for the years 2000-2019, with respect to the tropical-mean temperature at the same level between 30°N and 30°S according to the ERA5 reanalysis.

suggests that the deviations from strict WTG could be the result of gravity waves not eliminating all temperature gradients within the tropics. Other work has instead argued for the importance of balanced dynamics in the tropics (Raymond et al., 2015; Sessions et al., 2019; Adames, 2022), relating horizontal gradients in density to the balanced response to vorticity anomalies in the troposphere.

In contrast to the above mechanisms, convection has a strong effect on the temperature profile within a given column, providing a local, vertical control on the tropical thermal structure. Through the analysis of soundings from deep convective regions, it was suggested that the action of convection was to bring the vertical temperature profile towards neutrality with respect to a reversible, adiabatic ascent (Betts, 1982; Xu and Emanuel, 1989). Later studies, however, pointed out the sensitivity of this result to the inclusion of ice (Williams and Renno, 1993) and assumptions about microphysics (Bao and Stevens, 2021). Moreover, while undilute ascent within convective cores has previously been seen as an important process for explaining the observed tropical thermodynamic structure (Riehl and Malkus, 1958), observational studies near the end of last century provided evidence that undiluted air parcels are rare in the upper-troposphere (Jorgensen and LeMone, 1989; Lucas et al., 1994). Further observational studies pointed to a role of entrainment in determining cloud buoyancies in regions of moist convection (e.g. Zipser, 2003; Holloway and Neelin, 2009). In addition to this, idealised cloud-resolving studies (Kuang and Bretherton, 2006; Romps and Kuang, 2010) concluded that undilute air parcels in the upper-troposphere were too infrequent to be relevant. This then brought to question the effect the entrainment of environmental air would have on the tropospheric thermal structure.

To examine the impact of entrainment on the tropical temperature profile, Singh and O'Gorman (2013) introduced the conceptual zero-buoyancy plume (ZBP) model. Essentially, the model assumes that the aggregate effect of convection is to bring the temperature profile to one neutral to an entraining plume rather than a moist adiabat. While the model was originally applied to simulations of radiative-convective equilibrium as a model for the mean stratifica-

tion in the tropics, if applied locally to given columns, it suggests a connection between stability and humidity (Singh et al., 2019). In drier regions, entrainment has a stronger effect on rising air parcels, causing the environment to become more unstable. A number of studies have also reported that tropical lapse rates generally decrease as moisture in the troposphere increases (Singh and O'Gorman, 2013; Gjorgjievska and Raymond, 2014; Raymond et al., 2015), providing some evidence of a relationship between stability and moisture.

The importance of entrainment in moist convection has also been investigated from the inverse perspective, beginning by examining a relationship between convective activity and environmental conditions. It is well known that there is a strong relationship between precipitation and tropospheric moisture in the tropics (Bretherton et al., 2004; Holloway and Neelin, 2009). By considering the effect of convective entrainment, these relationships were framed in terms of the buoyancy of a hypothetical cloud that mixes with its environment by Ahmed and Neelin (2018). The authors used the observed precipitation-buoyancy relationship to motivate a model for the adjustment of temperature and moisture within the troposphere, finding a similar relationship between stability and humidity to that described by the ZBP model above (Ahmed et al., 2020).

Although there is some evidence for relationships between stability and humidity in the tropical atmosphere that are consistent with the ZBP model, the extent to which it is applicable at given locations in the tropics remains unclear. Singh et al. (2019) showed that the ZBP model performed well in reproducing the results of idealised cloud-resolving model simulations forced by varying degrees of ascent. However, as pointed out by Romps (2021), the simulations did not take into account WTG constraints on the tropical thermal structure and therefore could not be used as a proxy for observed spatial variations; the simulations implied horizontal gradients in temperature across the tropical band much larger than observed. Romps (2021) instead argued that horizontal controls from waves are too strong to allow the effect of entrainment to be observed in spatial variations in the lapse rate, but only in the tropical-mean lapse rate. A later study coupled the entraining plume model with a large-scale circulation to account for the dynamical constraints on the tropical atmosphere (Singh and Neogi, 2022). This study suggested that the ZBP could still be applied locally to the tropics, even under WTG constraints, thereby raising the possibility that the vertical control by tropical convection may partially explain deviations from strict WTG in the troposphere.

In this study, we investigate the horizontal and vertical influences on the thermal structure of the tropical troposphere using both reanalysis and observation data. We show that temperature profiles vary with mid-tropospheric humidity and that a relationship exists between stability and humidity in regions of convection. Within these regions, the ZBP model is able to reproduce the relationship for a sufficient entrainment rate, providing evidence that entrainment is an important factor in controlling local lapse rates within convecting regions. The same relationship is not observed in non-convective regions and further analysis reveals that local deviations from the WTG exist. Motivated by the "Circus Tents" model, we explore whether the lapse rates outside of convective regions can be understood as being set remotely by nearby convection. However, we find such an explanation to be too simple, and instead we highlight vertical variations in the efficacy of horizontal controls as an important avenue for future work.

The rest of the paper is organised as follows. The data used is described in Section 2. In Section 3 we examine the relationship between stability and humidity across the tropics and in Section 4 we compare these results to the ZBP model. We also study non-convective regions in Section 5 and investigate the local gradients in temperature between convective and non-convective regions. We present a summary and our main conclusions in section 6.

2 | DATA

The bulk of our analysis utilises the fifth generation of atmospheric reanalyses from the European Centre for Medium-range Weather Forecasts (ECMWF), ReAnalysis 5 (ERA5) (Hersbach et al., 2020). Data is provided on a 0.25x0.25 degree grid on 37 pressure levels at hourly time resolution, which we average to create daily means. We conduct our study over a twenty-year period (2000-2019) and focus on the region of the tropics between 20° N to 20° S.

We repeat the same analysis using the Modern-Era Retrospective analysis for Research and Application, Version 2 (MERRA2) (Global Modeling And Assimilation Office and Pawson, 2015a,b). MERRA2 has a 0.5x 0.625 degree grid available at 42 pressure levels. Once again, we look at a twenty-year period from 2000 to 2019 and focus on the region of the tropics between 20° N to 20° S. We average six hourly data for most variables to construct daily means, except for precipitation, for which we average hourly data to construct daily means.

Finally, we employ radiosonde and station data to examine whether the reanalysis results are supported by observational data. We use the Integrated Global Radiosonde Archive (IGRA) (Durre et al., 2016) for our free-tropospheric variables and combine this with observed station precipitation data from the Global Historical Climate Network (GHCN) (Menne et al., 2012). We analyse 71 stations between 20° N to 20° S that are featured in both IGRA and GHCN. When studying the data from the IGRA we take only soundings which provide temperature, humidity and height at 1000, 850, 700 and 500 hPa and discard soundings that do not contain all this data. We consider days for which there are at least two sounding launches, and we average all daily soundings together to construct an approximate daily mean. The GHCN contains daily data so no averaging for the data set was completed.

3 | EVIDENCE FOR A VERTICAL CONTROL ON THE THERMAL STRUCTURE IN CONVECTING REGIONS

We first examine relationships between stability and humidity in the tropical troposphere by compositing thermodynamic and dynamic profiles from ERA5 based on the lower-tropospheric moisture. We construct profiles of relative humidity, virtual temperature, and pressure vertical velocity anomalies as a function of the lower-tropospheric relative humidity (Fig. 2). Here the lower tropospheric relative humidity is taken as the weighted average of the humidity at pressure levels between 850 and 500 hPa.

The relative humidity throughout the column increases with the lower-tropospheric relative humidity (Fig. 2a), consistent with previous work demonstrating that variability in column humidity is driven by variations in the lower troposphere (Holloway and Neelin, 2009). In addition, the pressure velocity becomes increasingly negative, implying stronger upward motion, throughout the troposphere as the lower-tropospheric humidity increases (Fig. 2b), particularly for the highest relative humidity bin (90-100%). To the extent that large-scale upward motion is indicative of strong precipitation and convection (Louf et al., 2019), this is also consistent with much previous work on the relationship between humidity and precipitation in tropical regions (Bretherton et al., 2004; Holloway and Neelin, 2009; Rushley et al., 2018).

Interesting relationships are found between the lower-tropospheric relative humidity and the virtual temperature. The virtual temperature anomaly profiles vary strongly with humidity (Fig. 2c). However, in the lower-troposphere the variation is not monotonic. At low relative humidity, the virtual temperature anomaly is strongly negative at low levels, while for lower-tropospheric relative humidity values between 70-80% the anomalies are positive. At even higher lower-tropospheric relative humidity, the virtual temperature anomaly near the surface again becomes negative. At higher levels, different behaviour is seen; near 600 hPa, little variation in virtual temperature with humidity is seen,

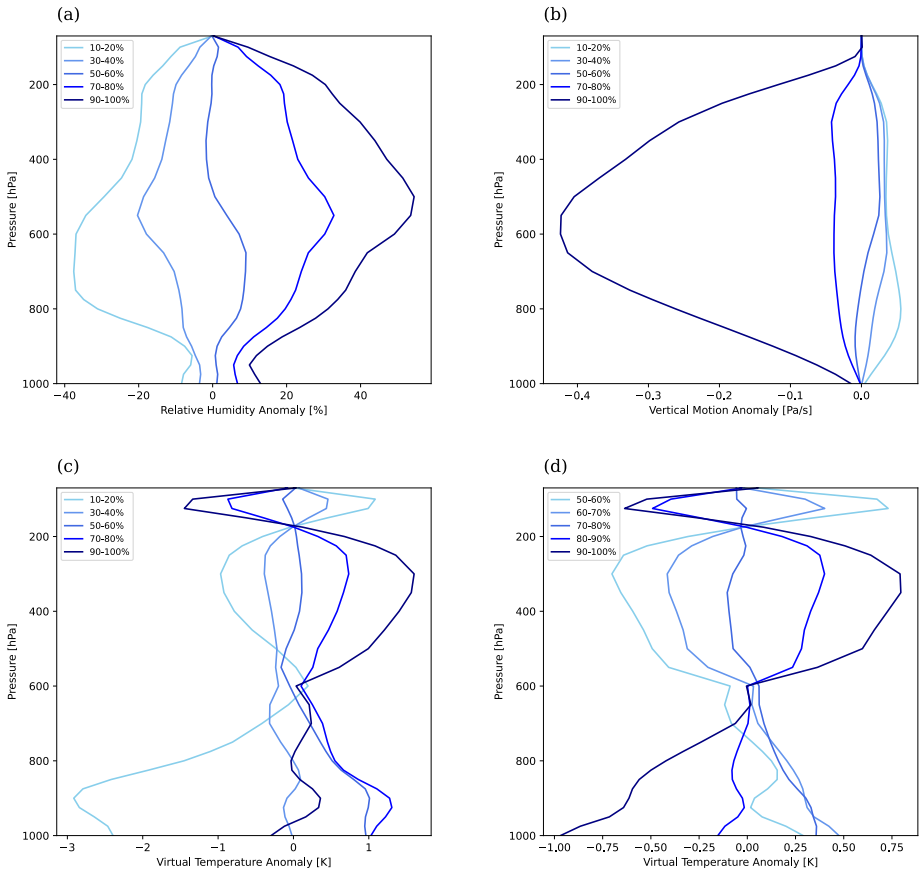

FIGURE 2 (a) Relative humidity anomalies, and (b) pressure velocity, (c), (d) virtual temperature anomalies binned by lower-tropospheric relative humidity according to ERA5. Lower-tropospheric relative humidity is taken as the pressure-weighted mean relative humidity between 850 and 500 hPa. Anomalies in (a), (b), (c) are taken with respect to the tropical and time mean and anomalies in (d) are taken with respect to the tropical and time mean for regions with lower-tropospheric relative humidity greater than 50%.

while above this level, the virtual temperature anomaly increases monotonically with humidity. Since the static stability within the troposphere is directly related to the change in virtual temperature with height, these results imply changes in the stability of the troposphere as a function of the relative humidity. Comparing virtual temperature anomalies in the lower- and upper-troposphere, the results suggest that the most unstable profiles occur under moderate relative humidity, with both the moistest and driest columns being more stable. In particular, for columns with humidities above 70%, corresponding to large-scale upward motion (Fig. 2b), the atmosphere becomes more stable as humidity increases.

The profiles seen above may be compared to the theoretical profiles described in Singh and Neogi (2022). They developed a model for the thermodynamic and dynamic structure of the ascending branch of a large-scale circulation using the ZBP model coupled to a dynamic model based on the WTG approximation. In particular, they showed that the ascending branch has a higher tropospheric relative humidity than the tropical mean, and temperature anomalies that are negative at low levels and positive at high levels, implying a more stable troposphere than the tropical mean. Indeed a similar profile of virtual temperature anomalies is produced in the ascent region when we consider only regions of the atmosphere in which the lower-tropospheric relative humidity is greater than 50% (Fig. 2d); moister regions have negative anomalies below 850 hPa and positive anomalies of virtual temperature above 400 hPa. The virtual temperature profiles found in ERA5 are therefore qualitatively consistent with the behaviour of the ZBP model, in which entrainment plays a key role in setting the lapse rate, motivating us to apply this model to help explain the reanalysis data in the next section.

4 | COMPARISON TO THE ZERO-BUOYANCY PLUME MODEL

The ZBP model assumes that the environment of convection adjusts to a state neutral to an entraining plume. Neglecting virtual effects, this implies that the saturation moist static energy (MSE^*) of the troposphere above cloud base obeys the plume equation,

$$\frac{dMSE^*}{dz} = -\epsilon L_v (q^* - q) \tag{1}$$

where ϵ is the entrainment rate, $MSE^* = c_p T + gz + L_v q^*$ is the saturation moist static energy, $q^* - q$ is the saturation deficit and z is height. Here c_p is the isobaric specific heat capacity of air, L_v is the latent heat of vaporization, T is the temperature, q is the specific humidity, q^* is the saturation specific humidity, and g is the gravitational acceleration. Integrating in the vertical between two levels, we may write

$$\Delta MSE^* = -\epsilon \Delta z L_v \overline{(q^* - q)} \tag{2}$$

Where ΔMSE^* is the change in MSE between the two levels separated by a height difference Δz, and the overbar represents a height-weighted mean.

The above equation implies that the vertical change in MSE^* is directly related to the saturation deficit. MSE^* is a function of temperature, pressure and height only, and so its variation in the vertical is a measure of stability. If MSE^* is invariant with height, the stability is moist adiabatic, whereas if it decreases with height, the atmosphere is more unstable than a moist adiabat. The saturation deficit, on the other hand, is a measure of humidity, with zero saturation deficit implying saturated conditions. In this way, the ZBP model implies a relationship between stability and humidity. We focus here on the mid- to lower-troposphere, and we consider the interval between 850 hPa and

500 hPa.

Figure 3 shows solutions of (2) for three different entrainment rates of 0.1, 0.25 and 0.5 km^{-1} based on a height difference of approximately 4 km, given by the average height difference between 850 and 500 hPa in the tropical band (20°S-20°N) in ERA5. The model predicts a linear relationship between the stability (as measured by ΔMSE^*) and the humidity (as measured by the saturation deficit). For zero saturation deficit, entrainment has no effect on the ZBP, and ΔMSE^* is zero.

We can now compare the ZBP solutions to data from ERA5 and the IGRA. We calculate MSE^* from daily-averaged profiles of temperature and geopotential height over the interval 850 to 500 hPa. We evaluate the saturation deficit over the same region using a height-weighted average, and we multiply by the latent heat of vaporisation to convert to energy units.

We construct a 2D histogram, plotting the values of the change in MSE^* against the corresponding saturation deficit and overlaying the ZBP solutions onto the ERA5 distribution. Immediately, there is a clear correlation between the change in MSE^* and the saturation deficit, where more instability occurs in regions and at times where the troposphere is drier (Fig. 3a). Although there is considerable scatter in the points, for small values of the saturation deficit there appears to be a relatively linear relationship between ΔMSE^* and saturation deficit, aligning with the ZBP solution for an entrainment rate of roughly 0.25 km^{-1}.

To determine whether a similar relationship is found in direct observations, we construct the same histogram based on the IGRA radiosonde data. There is considerably more scatter in the points, and any relationship is less clear. This is partly simply because of the lack of data; only 68 stations are available in the 20°N-20°S, and this gives a total number of profiles of 240515 compared to 1.68 billion in ERA5. Additionally, since the radiosondes give point measurements rather than averages, the humidity they measure may not be representative of the average environment for convection, and may be moister or drier. This could lead to more scatter in the histogram, even if the fundamental relationship is present in the observed data.

Despite the above caveats, the region of highest frequencies of occurrence tends to be elongated along the ZBP solution of 0.25 km^{-1}. Thus though not conclusive, the results suggest that the humidity-stability relationship found in ERA5 is not simply an artifact of the reanalysis. Note that the saturation deficit values for the radiosonde data appear to be generally higher than those for the reanalysis. This is due to differences between the distribution of saturation deficit between the observations and the reanalysis, with the radiosondes leaning towards larger saturation deficits. It is possible that an actual difference in these values exists between the soundings and reanalysis, although it may also be due to the single point values in the soundings differing to the area average in the ERA5 reanalysis.

Finally, we also computed the stability-humidity histogram in a second reanalysis (MERRA2). Although the entrainment values that encompassed the data appear slightly different to those for ERA5, the overall relationship remains clear (Fig. 3e, f).

At higher values of the saturation deficit, the spread in the data becomes larger, and the relationship between MSE^* and the saturation deficit deviates from that predicted by the ZBP model. One possible reason for this is that the ZBP model is only properly representative of convective regions. Since the ZBP model assumes that the atmosphere is rapidly brought to neutrality with respect to convection, it is only valid where convection is active. We therefore examine how the histogram is altered if we only consider regions where moist convection is present. We use total precipitation in ERA5 (convective and large-scale) as a proxy for convection and set a threshold of 5 mm/day to exclude regions where moist convection is not occurring. With this idea now in mind, we plot the ERA5 distribution including only regions that exceed the precipitation threshold (Fig. 3b). With precipitation generally occurring in more moist atmospheres this removes much of the scatter of the distribution observed at values of greater saturation deficit. The resulting figure now has a very strong linear relationship between the change in MSE^* and the saturation deficit

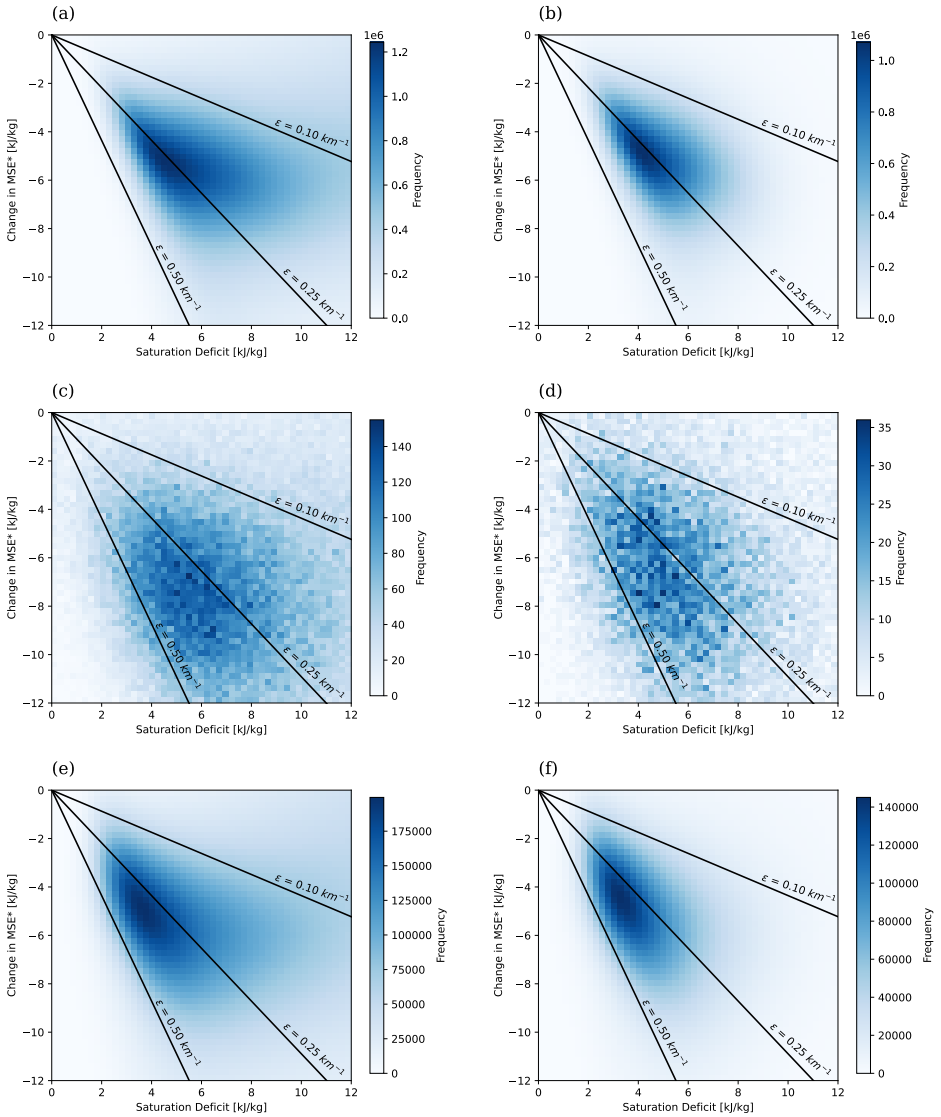

FIGURE 3 2D histograms depicting the relationship between the change in MSE* and the saturation deficit between 850 hPa and 500 hPa. Solid black lines give solutions of the ZBP model for varying entrainment rates as labelled. (a), (b) are the results from ERA5, (c), (d) are the results from the IGRA radiosonde data and (e), (f) are the results from MERRA2. (a), (c), (e) include all points with the domain (20°N-20°S) and (b), (d), (f) include only points exceeding the precipitation threshold of 5mm/day.

across all values of humidity.

When we consider only precipitating regions in the radiosonde data, as given by a daily precipitation rate larger than 5mm according to the GHCN database, the histogram appears slightly more aligned with the ZBP solutions, but remains relatively unchanged. The reasons for this are possibly to do with the lack of data and representation errors discussed earlier.

Based on the above results, we suggest that while the ZBP model provides and explanation for some of the variation in lapse rates in regions of precipitation, it performs poorly at explaining relationships between stability and humidity outside these regions. In non-precipitating regions it is likely that horizontal controls on the thermal structure can effectively inhibit differences in stability between regions of varying humidity. We now investigate these horizontal controls in more detail.

5 | HORIZONTAL CONTROLS ON THE THERMAL STRUCTURE IN NON-CONVECTIVE REGIONS

The conceptual "Circus Tents" model introduced by Williams et al. (2023) suggests that MSE* in the free-troposphere is communicated horizontally via gravity waves from convective to non-convective regions. This establishes a threshold for convection for regions in the vicinity of active convection, so that convection cannot occur unless the MSE in the sub cloud layer is equal to or greater than the communicated value of free-tropospheric MSE*. Whilst according to this model the threshold for convection decreases with distance from the active convection, we can expect that non-convective regions nearby would have roughly similar MSE* to the convective area. Therefore, according to this theory, the change in MSE* between 850 hPa and 500 hPa should be somewhat similar between convective and non-convective regions that are located close to one another.

Using this knowledge, we can test the extent of this horizontal control on the thermal structure for non-convective regions. If we expect non-precipitating regions near precipitating regions to have similar values of stability in the mid- to lower-troposphere, the stability of the non-precipitating regions should still follow the ZBP model, but with the relative humidity given by the nearby convective regions. That is, we expect a correlation between the stability in the non-precipitating region and the humidity of the nearby precipitating regions to be present.

We choose points that do not reach the precipitation threshold of 5 mm/day to be our non-precipitating regions. The next step is then to look at all precipitating regions within some set distance from a given non-precipitating grid point and take the average saturation deficit of these regions. We select a distance radius of 500 km, where any precipitating points within this distance to a non-precipitating point between 20° N to 20° S are included in the average. To observe the change this has on the distribution we plot both the unaltered saturation deficit of non-precipitating regions that have at least one point of precipitation within 500 km, and then the corresponding distribution but with the average saturation deficit altered to be the mean of the nearby precipitating regions. Lastly, we plot the same values as the altered humidity data set, but here we randomise the values for saturation deficit associated with each value of change in MSE*. This acts as a control, representing a distribution that would depict no correlation to the change in MSE* of nearby precipitating points, and therefore no horizontal communication of these values of stability.

The resulting distribution of this experiment depicted in Figure 4 is intriguing. It is clear that by altering the saturation deficit, the distribution has shifted to the left from the originally dry distribution. The centre contour representing 10% of the data has turned so that its slope is somewhat comparable to the precipitating distribution shown in Fig. 3. However, as we turn our attention to more of the data, the altered humidity distribution has a wide

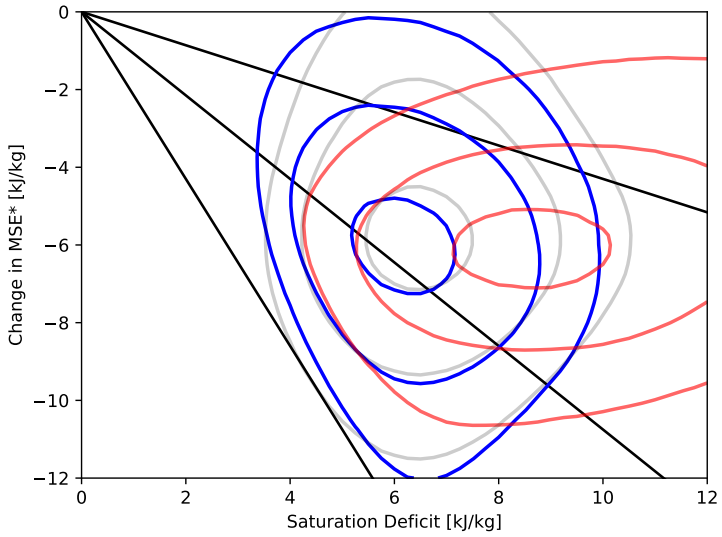

FIGURE 4 Contour plot depicting the relationship in ERA5 between the change in MSE* and the saturation deficit between 850 hPa and 500 hPa for non-precipitating regions. The unaltered saturation deficits are enclosed by the red contours. The blue contours enclose the distribution where the saturation deficits have been altered to be equal to the average saturation deficit of precipitating points within 500 km of each non precipitating point. The grey contours depict a control relationship where the data enclosed within the blue contours has been shuffled so that no relationship between humidity and stability exists. The contours enclose 10%, 50% and 80% of each data set. The ZBP solutions for different entrainment rates of 0.1 km^{-1}, 0.25 km^{-1} and 0.5 km^{-1} are plotted in black with increasing entrainment from top to bottom

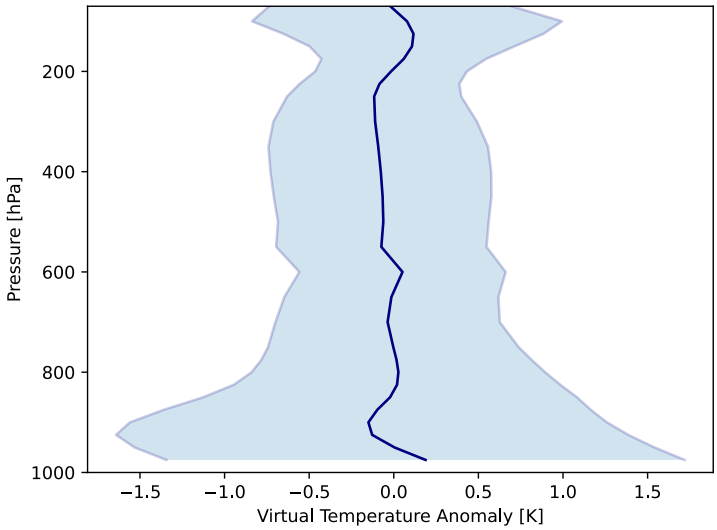

FIGURE 5 The average vertical profile (solid blue line) of the difference in virtual temperature between non-precipitating regions and precipitating regions within 500 km of each non-precipitating point. Light blue shading shows one standard deviation from the mean.

spread, and is in fact relatively similar to the control distribution, suggesting no relationship between local stability and the humidity of nearby convecting regions.

A few reasons for this result could be possible. Firstly, our assumption that the MSE* between precipitating and non-precipitating regions was similar enough to be simplified to being equal could be incorrect. We did not account for a decrease in the communicated value of MSE* from convective to non-convective regions, which perhaps is significant enough to account for a clear distribution not being observed when neglecting this. On the other hand, the set distance radius of 500 km may be too large or too small. To test this, we constructed the same plot as Figure 4, but using distances of 120 km and 1000 km. At the larger range of 1000 km, the distribution was very similar to the control, suggesting that this range is too large to consider MSE* equal between non-precipitating and precipitating regions. At 120 km the distribution was least similar to the control, however a slope similar to the precipitating regions was not found.

Finally, another theorised reason for this was that whilst MSE* in the mid-troposphere may be similar between precipitating and non-precipitating regions, this may not be the case in the lower-troposphere. This would imply that the change in MSE* between 500 hPa and 850 hPa may not be comparable between two such regions. As pointed out by Bao and Stevens (2021), the efficacy of gravity waves to reduce temperature gradients differs throughout the troposphere. Gravity waves may therefore be more efficient at reducing temperature gradients at 500 hPa compared to 850 hPa, which is closer to the boundary layer. To test this theory, we can examine the spread in temperature differences between non-precipitating and the precipitating points that are within 500 km. To focus on differences in density, we compare the virtual temperature between the two regions. Specifically, we consider the profile of differences in virtual temperature between non-precipitating grid points and precipitating grid points within 500 km (Fig. 5).

In the mean, temperature gradients are mostly removed locally between precipitating and non-precipitating regions at all levels in the troposphere. However, when we examine the standard deviation of the temperature differences, there is more variation in the lower-troposphere than there is in the mid- to upper-troposphere. As well as this, the standard deviation also implies that locally temperature gradients persist between precipitating and non-precipitating points at a 500 km scale, with differences ranging from ± 1.5 K in the lower troposphere to ± 0.5 K in the upper troposphere. Therefore, due to these two points, we cannot assume that the change in MSE^* between 500 hPa and 850 hPa is equivalent between precipitating and non-precipitating points at this scale.

These results demonstrate that QE is not a good approximation for non-precipitating regions because of the absence of moist convection. As well as this, a strict WTG cannot be used to precisely approximate the thermal structure of non-precipitating points. As depicted in Figure 5, deviations from strict WTG exist at local scales and the magnitude of these deviations varies with height. Therefore, it can be concluded that understanding the deviations from the WTG, as well as how these depend on height, is important for understanding the thermal structure of regions outside of moist convection.

6 | CONCLUSION

In this study we have investigated how both the horizontal and vertical controls on the thermal structure of the tropical troposphere affect stability and its variations. Vertical profiles of virtual temperature for varying mid-tropospheric humidities demonstrated a variation in thermal stratification with environmental moisture. This was also shown to be non-monotonic in the lower-troposphere, but monotonic above 600 hPa. Further investigating the influence of moist convection on stability, we identified a relationship between stability and humidity in precipitating regions, with greater instability present in drier atmospheres. The ZBP model was also able to reproduce the slope of the relationship between the two variables with an entrainment rate of 0.25 km^{-1}. However, this relationship was not present in non-precipitating regions and therefore, the ZBP cannot be applied to describe the thermal structure in such regions. The absence of this relationship was theorised to be caused by the reduction of temperature gradients via gravity waves. Whilst on average, temperature differences between non-convecting and nearby convecting regions are small, there was considerable variability, and this variability had larger magnitude in the lower-troposphere compared to the mid-troposphere.

Our results provide evidence for entrainment impacting the thermal structure, and thereby also provide evidence that ascent within convective clouds is far from being moist adiabatic. In addition, our results also provide support for the local applicability of the ZBP model to regions of convection within the tropics. Whilst this model captures the potential cause for the deviations from strict moist neutrality in convecting regions, the mechanisms controlling horizontal temperature gradients in non-convecting regions are less obvious. We have highlighted the existence of local temperature gradients which supports the conceptual "Circus Tents" model (Williams et al., 2023). However, our results could be interpreted to suggest that the rate at which the communicated value of MSE^* decreases away from convective regions may vary with height in the troposphere. The efficacy of gravity waves has been suggested to cause the deviation from a strict WTG (Bao and Stevens, 2021), however this does not explain what sets the local thermal structure. There may then be other factors involved in controlling stability in non-convective regions, including balanced dynamics involving the rotational component of the winds (Adames, 2022).

While we have focused on entrainment as a key explanation for the relationships between stability and humidity seen in our study, alternative mechanisms that may contribute to this relationship should be mentioned. In particular, variations in convective organisation with humidity may play an important role in setting variations in stability across

convective regions. This may occur through variations in entrainment induced by organisation (Becker et al., 2018), but it may also occur due to different vertical profiles of convective heating associated with organised convection compared to disorganised convection (e.g., Houze Jr (1989)). Additionally, differences in cloud-radiative heating may play a similar role and also affect the stratification differently in different regions. However, both of these mechanisms are likely to be most important in the upper-troposphere, while we have here focused mainly on the lower-troposphere to mid-troposphere.

Despite our lower-tropospheric focus, our results may nevertheless be relevant for the temperature structure of the upper-troposphere. For example, climate models are known to overestimate upper-tropospheric temperature trends relative to radiosondes and satellite observations (Miyawaki et al., 2020; Keil et al., 2021). One possible mechanism that would lead to this overestimation is an incorrect representation of entrainment in moist convection (Miyawaki et al., 2020). Our results therefore provide a possible observational constraint on convective entrainment that could be used to test this hypothesis. Alternative constraints on convective mixing have previously been proposed by Ahmed and Neelin (2018). A possible pathway for future work is therefore to examine the stability-saturation deficit phase space within climate models, and explore the implications for models that are unable to reproduce the reanalysis results found here.

Finally, an important open question is to understand the causes of horizontal temperature gradients in the tropical atmosphere in regions far from convection. Previous work has related such gradients to the momentum budget (Bao et al., 2022), balanced dynamics (Adames, 2022), and the linear response to convective heating (Keil et al., 2023) but a simple model such as the “Circus Tents" model that can provide quantitative predictions of gradients remains elusive.

Author Contributions

L. A. Palmer: conceptualisation; formal analysis; investigation; methodology; visualisation; writing - original draft; writing - review and editing. **M. S. Singh:** conceptualisation; investigation; methodology; supervision; writing - review and editing

Acknowledgements

We acknowledge the European Centre for Medium-Range Weather Forecasts, which is responsible for ERA5, as well as the National Aeronautics and Space Administration, which is responsible for MERRA2. We also acknowledge the National Centers for Environmental Information, which is responsible for IGRA and GHCN. We acknowledge support from the Australian Research Council and the Centre of Excellence for Climate Extremes, as well as computational resources and services from the National Computational Infrastructure, all funded by the Australian Government. Open access publishing facilitated by Monash University, as part of the Wiley – Monash University agreement via the Council of Australian University Librarians.

Conflict of Interest

The authors declare no conflict of interest.

Data Availability Statement

The European Centre for Medium-Range Weather Forecasts ERA5 reanalysis dataset used in this study is available at `https://cds.climate.copernicus.eu/cdsapp#!/dataset/reanalysis-era5-complete?tab=form`. The Modern-Era Retrospective analysis for Research and Application, Version 2 (MERRA2) reanalysis dataset used is available at `https://disc.gsfc.nasa.gov/datasets?project=MERRA-2`. The Integrated Global Radiosonde Archive (IGRA) data used is available at `https://www.ncei.noaa.gov/data/integrated-global-radiosonde-archive/access/data-por/` and the Global Historical Climate Network (GHCN) dataset used is available at `https://www.ncei.noaa.gov/data/global-historical-climatology-network-daily/access/`. Scripts and programming used for the analysis in the current study are available from the author upon request.

references

Adames, Á. F. (2022) The Basic Equations under Weak Temperature Gradient Balance: Formulation, Scaling, and Types of Convectively Coupled Motions. *Journal of the Atmospheric Sciences*, **79**, 2087–2108.

Ahmed, F., Adames, Á. F. and Neelin, J. D. (2020) Deep convective adjustment of temperature and moisture. *Journal of the Atmospheric Sciences*, **77**, 2163–2186.

Ahmed, F. and Neelin, J. D. (2018) Reverse Engineering the Tropical Precipitation–Buoyancy Relationship. *Journal of the Atmospheric Sciences*, **75**, 1587–1608.

Bao, J., Dixit, V. and Sherwood, S. C. (2022) Zonal Temperature Gradients in the Tropical Free Troposphere. *Journal of Climate*, **35**, 7937–7948.

Bao, J. and Stevens, B. (2021) The Elements of the Thermodynamic Structure of the Tropical Atmosphere. *Journal of the Meteorological Society of Japan. Ser. II*, **99**, 1483–1499.

Becker, T., Bretherton, C. S., Hohenegger, C. and Stevens, B. (2018) Estimating bulk entrainment with unaggregated and aggregated convection. *Geophysical Research Letters*, **45**, 455–462.

Betts, A. K. (1982) Saturation Point Analysis of Moist Convective Overturning. *Journal of the Atmospheric Sciences*, **39**, 1484–1505.

Bretherton, C. S., McCaa, J. R. and Grenier, H. (2004) A New Parameterization for Shallow Cumulus Convection and Its Application to Marine Subtropical Cloud-Topped Boundary Layers. Part I: Description and 1D Results. *Monthly Weather Review*, **132**, 864–882.

Bretherton, C. S. and Smolarkiewicz, P. K. (1989) Gravity Waves, Compensating Subsidence and Detrainment around Cumulus Clouds. *Journal of the Atmospheric Sciences*, **46**, 740–759.

Charney, J. G. (1963) A Note on Large-Scale Motions in the Tropics. *Journal of the Atmospheric Sciences*, **20**, 607–609.

Durre, I., Yin, X., Vose, R. S., Applequist, S., Arnfield, J., Korzeniewski, B. and Hundermark, B. (2016) Integrated Global Radiosonde Archive (IGRA), Version 2.

Gjorgjievska, S. and Raymond, D. J. (2014) Interaction between dynamics and thermodynamics during tropical cyclogenesis. *Atmospheric Chemistry and Physics*, **14**, 3065–3082.

Global Modeling And Assimilation Office and Pawson, S. (2015a) MERRA-2 inst6_3d_ana_np: 3d,6-Hourly,Instantaneous,Pressure-Level,Analysis,Analyzed Meteorological Fields V5.12.4.

— (2015b) MERRA-2 tavg1_2d_flx_nx: 2d,1-Hourly,Time-Averaged,Single-Level,Assimilation,Surface Flux Diagnostics V5.12.4.

Hersbach, H., Bell, B., Berrisford, P., Hirahara, S., Horányi, A., Muñoz-Sabater, J., Nicolas, J., Peubey, C., Radu, R., Schepers, D., Simmons, A., Soci, C., Abdalla, S., Abellan, X., Balsamo, G., Bechtold, P., Biavati, G., Bidlot, J., Bonavita, M., De Chiara, G., Dahlgren, P., Dee, D., Diamantakis, M., Dragani, R., Flemming, J., Forbes, R., Fuentes, M., Geer, A., Haimberger, L., Healy, S., Hogan, R. J., Hólm, E., Janisková, M., Keeley, S., Laloyaux, P., Lopez, P., Lupu, C., Radnoti, G., De Rosnay, P., Rozum, I., Vamborg, F., Villaume, S. and Thépaut, J. (2020) The ERA5 global reanalysis. *Quarterly Journal of the Royal Meteorological Society*, **146**, 1999–2049.

Holloway, C. E. and Neelin, J. D. (2009) Moisture Vertical Structure, Column Water Vapor, and Tropical Deep Convection. *Journal of the Atmospheric Sciences*, **66**, 1665–1683.

Houze Jr, R. A. (1989) Observed structure of mesoscale convective systems and implications for large-scale heating. *Quarterly Journal of the Royal Meteorological Society*, **115**, 425–461.

Jorgensen, D. P. and LeMone, M. A. (1989) Vertically Velocity Characteristics of Oceanic Convection. *Journal of the Atmospheric Sciences*, **46**, 621–640.

Keil, P., Schmidt, H., Stevens, B. and Bao, J. (2021) Variations of Tropical Lapse Rates in Climate Models and their Implications for Upper Tropospheric Warming. *Journal of Climate*, **34**, 9747–9761.

Keil, P., Schmidt, H., Stevens, B., Byrne, M. P., Segura, H. and Putrasahan, D. (2023) Tropical tropospheric warming pattern explained by shifts in convective heating in the matsuno–gill model. *Quarterly Journal of the Royal Meteorological Society*, **149**, 2678–2695.

Kuang, Z. (2008) Modeling the interaction between cumulus convection and linear gravity waves using a limited-domain cloud system-resolving model. *J. Atmos. Sci.*, **65**, 576–591.

Kuang, Z. and Bretherton, C. S. (2006) A Mass-Flux Scheme View of a High-Resolution Simulation of a Transition from Shallow to Deep Cumulus Convection. *Journal of the Atmospheric Sciences*, **63**, 1895–1909.

Louf, V., Jakob, C., Protat, A., Bergemann, M. and Narsey, S. (2019) The Relationship of Cloud Number and Size With Their Large-Scale Environment in Deep Tropical Convection. *Geophysical Research Letters*, **46**, 9203–9212.

Lucas, C., Zipser, E. J. and LeMone, M. A. (1994) Convective Available Potential Energy in the Environment of Oceanic and Continental Clouds: Correction and Comments. *Journal of the Atmospheric Sciences*, **51**, 3829–3830.

Mapes, B. E. (2001) Water's two height scales: The moist adiabat and the radiative troposphere. *Quarterly Journal of the Royal Meteorological Society*, **127**, 2353–2366.

Menne, M. J., Durre, I., Korzeniewski, B., McNeill, S., Thomas, K., Yin, X., Anthony, S., Ray, R., Vose, R. S., Gleason, B. E. and Houston, T. G. (2012) Global Historical Climatology Network - Daily (GHCN-Daily), Version 3.

Miyawaki, O., Tan, Z., Shaw, T. A. and Jansen, M. F. (2020) Quantifying Key Mechanisms That Contribute to the Deviation of the Tropical Warming Profile From a Moist Adiabat. *Geophysical Research Letters*, **47**, e2020GL089136.

Raymond, D., Fuchs, Ž., Gjorgjievska, S. and Sessions, S. (2015) Balanced dynamics and convection in the tropical troposphere. *Journal of Advances in Modeling Earth Systems*, **7**, 1093–1116.

Raymond, D. J. and Zeng, X. (2005) Modelling tropical atmospheric convection in the context of the weak temperature gradient approximation. *Quarterly Journal of the Royal Meteorological Society*, **131**, 1301–1320.

Riehl, H. and Malkus, J. S. (1958) On the Heat Balance in the Equatorial Trough Zone. *Geophysica*, **6**, 503–538.

Romps, D. M. (2021) Ascending Columns, WTG, and Convective Aggregation. *Journal of the Atmospheric Sciences*, **78**, 497–508.

Romps, D. M. and Kuang, Z. (2010) Nature versus Nurture in Shallow Convection. *Journal of the Atmospheric Sciences*, **67**, 1655–1666.

Rushley, S. S., Kim, D., Bretherton, C. S. and Ahn, M. (2018) Reexamining the Nonlinear Moisture-Precipitation Relationship Over the Tropical Oceans. *Geophysical Research Letters*, **45**, 1133–1140.

Sessions, S. L., Sentić, S. and Raymond, D. J. (2019) Balanced Dynamics and Moisture Quasi-Equilibrium in DYNAMO Convection. *Journal of the Atmospheric Sciences*, **76**, 2781–2799.

Singh, M. S. and Neogi, S. (2022) On the Interaction between Moist Convection and Large-Scale Ascent in the Tropics. *Journal of Climate*, **35**, 4417–4435.

Singh, M. S. and O'Gorman, P. A. (2013) Influence of entrainment on the thermal stratification in simulations of radiative-convective equilibrium. *Geophysical Research Letters*, **40**, 4398–4403.

Singh, M. S., Warren, R. A. and Jakob, C. (2019) A Steady-State Model for the Relationship Between Humidity, Instability, and Precipitation in the Tropics. *Journal of Advances in Modeling Earth Systems*, **11**, 3973–3994.

Sobel, A. H., Nilsson, J. and Polvani, L. M. (2001) The Weak Temperature Gradient Approximation and Balanced Tropical Moisture Waves. *Journal of the Atmospheric Sciences*, **58**, 3650–3665.

Williams, A. I. L., Jeevanjee, N. and Bloch-Johnson, J. (2023) Circus Tents, Convective Thresholds, and the Non-Linear Climate Response to Tropical SSTs. *Geophysical Research Letters*, **50**, e2022GL101499.

Williams, E. and Renno, N. (1993) An Analysis of the Conditional Instability of the Tropical Atmosphere. *Monthly Weather Review*, **121**, 21–36.

Xu, K.-M. and Emanuel, K. A. (1989) Is the Tropical Atmosphere Conditionally Unstable? *Monthly Weather Review*, **117**, 1471–1479.

Yang, D., Zhou, W. and Seidel, S. D. (2022) Substantial influence of vapour buoyancy on tropospheric air temperature and subtropical cloud. *Nature Geoscience*, **15**, 781–788.

Zipser, E. J. (2003) Some Views On "Hot Towers" after 50 Years of Tropical Field Programs and Two Years of TRMM Data. In *Cloud Systems, Hurricanes, and the Tropical Rainfall Measuring Mission (TRMM)* (eds. W.-K. Tao and R. Adler), 49–58. Boston, MA: American Meteorological Society.

GRAPHICAL ABSTRACT

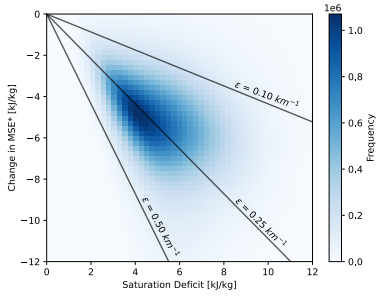

Our conceptual understanding of the tropical thermal structure is based on two complementary idealisations: convective quasi-equilibrium (QE) and the weak-temperature gradient (WTG) approximation We discover that, in convective regions, moist convection is most influential and that the resulting relationship between stability and humidity can be well approximated by an entraining plume model. However, in non-convective regions, QE cannot be used to explain the thermal structure and instead the WTG, and possibly other factors, act to set stability in the region.

The Horizontal and Vertical Controls on the Thermal Structure of the Tropical Tropopshere

L. A. Palmer* and M. S. Singh

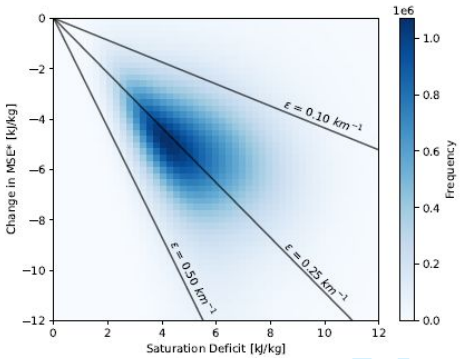

Our conceptual understanding of the tropical thermal structure is based on two complementary idealisations: convective quasi-equilibrium (QE) and the weak-temperature gradient (WTG) approximation We discover that, in convective regions, moist convection is most influential and that the resulting relationship between stability and humidity can be well approximated by an entraining plume model. However, in non-convective regions, QE cannot be used to explain the thermal structure and instead the WTG, and possibly other factors, act to set stability in the region.

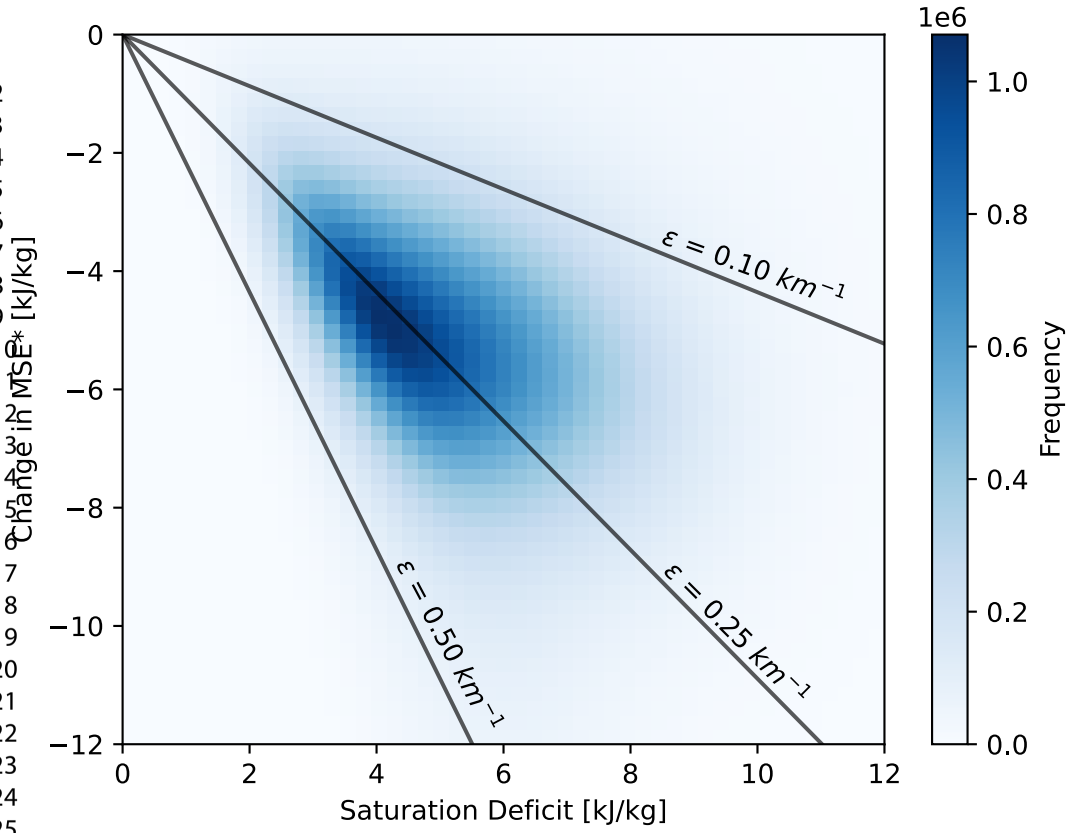
Change in MSE* [kJ/kg]
Saturation Deficit [kJ/kg]
Frequency
1e6
ε = 0.10 km⁻¹
ε = 0.25 km⁻¹
ε = 0.50 km⁻¹
0
−2
−4
−6
−8
−10
−12
0
2
4
6
8
10
12
1.0
0.8
0.6
0.4
0.2
0.0